JMES The International Journal of Mechanical Engineering and Sciences
https://iptek.its.ac.id/index.php/jmes
e-ISSN 2580-7471

Numerical Study of Deflection and Stress Distribution on Composite Box Spar Structure – Application in Wind Turbine Blade

Putri Safina Ufaira[1*], Putu Suwarta[1], Galih Bangga[2]

[1]Department of Mechanical Engineering, Institut Teknologi Sepuluh Nopember, Surabaya 60111, Indonesia
[2]Institute of Aerodynamics and Gas Dynamics, University of Stuttgart, 70569 Stuttgart, Germany

Received: 30 August 2021, Revised: 23 March 2022, Accepted: 28 March 2022

Abstract

This paper present finite element analysis on the internal structure of wind turbine to examined the deflection and stress distribution. The structure was modeled as a cantilever box beam with constant cross section along the length. The dimension of the structure was set according to the original design of the 10 MW AVATAR (Advanced Aerodynamic Tools for Large Rotors) wind turbine. The proposed materials were unidirectional thin-ply TC35/Epoxy and M55/Epoxy carbon composites and standard thickness S−Glass 913/Epoxy composite. The fibre at the spar caps is oriented at 90° and at the shear webs at 0°. The deflection curve of the three composite materials showing non-linear behaviour with a maximum deflection of 2.618 m, 2.429 m, 4.175 m at the blade tip for S−Glass 913/Epoxy, T35/Epoxy, M55/Epoxy respectively which is less than the maximum deflection of an existing AVATAR beam. The critical stresses are located at the top outer surface of the spar cap which received the load directly and at the intersection between the spar caps and shear webs where stress transfer occurs. The deflection performance of the structure is dictated by the transverse Young's Modulus (E_{22}) while the longitudinal Young's Modulus (E_{11}) plays an important role on stress distribution.

Keywords: Box spar, carbon fibre composite, glass fibre composite, deflection, stress distribution, wind turbine blade

1. Introduction

Global energy consumption is expected to increase to about 21% every year according to IEA (International Energy Agency) [1]. To meet this great demand of energy and due to increased people awareness to clean energy resources, wind energy has become one of prominent players in the market in several countries. Wind turbine works by converting kinetic energy from wind power into electricity through generator. As power output of wind turbine is proportional to the wind power, it is important to consider the characteristic of wind power where its speed varies from time to time.

Increasing wind power can be done by using a larger blade to produce bigger swept area. It is also known that the stiffness of the blade is influenced by the components of the blade itself including airfoil shell, shear web and spar flanges. The latter two components especially contribute significantly to the stiffness of the blade. These are mainly to withstand the loads from the flapwise and edgewise moments. This first load component acts in the direction of wind while the latter is in the direction of rotor rotation. The flapwise component could be 100 times larger than the edgewise component depending on the case. This has been shown for example by Bangga both using engineering model [2] and high fidelity CFD (computational fluid dynamics) computations [3]. Therefore, it is logical to focus more into the flapwise component of the loads.

According to Ghasemi [4] with bigger blades, inertia forces will dominate more compared to aerodynamics, it is then needed to use material with good strength-to-weight ratio like composite materials. GFRP (glass fiber-reinforced polymer) and CFRP (carbon fiber-reinforced polymer) are the prime examples of the most commonly employed materials for wind turbine blades. Numerous studies regarding composite materials and the structural dynamics of wind turbine blades have been done in the past. For instance Veers et al. [5] highlighted that GFRP and CRFP are two most commonly used for wind turbine blades. Cox and Echtermeyer [6] investigated the deflection characteristics of a 10 MW turbine having a radius of 70 m. To add further, Prombut and Anakpotchanakul [7] also demonstrated that the way composite material is aligned could be important for deflection characteristics.

Above literature review has shown that composite material is an important player in wind turbine blade design. Various studies have been conducted on common material such as GFRP and CFRP but limited amount of

*Corresponding author. Email: safina.ufaira@gmail.com.

effort is only given for a new composite material namely thin-ply M55 carbon/epoxy, thin-ply TC35 carbon/epoxy and standard thickness S−Glass 913/epoxy. The studies will be conducted numerically employing a finite element analyses with the help of a software package ABAQUS. The structural response of each composite material will be presented in the present studies. The paper is organized as follows. Section 2 describes the computational modeling and the simplification of the turbine blade geometry. In Section 3, the results will be presented and discussed thoroughly, and all the results will be concluded in Section 4.

2. Method

2.1. Computational Model

The geometry used refers to AVATAR wind turbine research [8] and INNWIND [9] designs. Some simplifications were made for this study. The blade of wind turbine consists of airfoil as an outer structure and an internal structure commonly modeled as box or O beam. In this study, the internal structure was modeled as cantilever box spar consisting of spar caps and shear webs with constant cross section along the span. In an initial structural study, it is assumed that the performance of internal structure could represent the whole structural performance of wind turbine blade [10]. The airfoil section was ignored for model simplification and since the exact coordinates of the airfoils are not yet reported. The box spar was partitioned into four parts for the stress distribution analysis. The model is illustrated in Figure 1 according to the dimension given in Table 1. It is should be noted that The fibre direction at the spar cap is arranged at 90° relative to the loading direction while at the shear web, the fibre is arranged at 0° relative to the loading direction.

It can be seen from Table 1 that spar caps and shear webs have different width and thickness, with spar caps being on the larger side. 102.88 meters-long box spar was designed in ABAQUS as a solid beam with continuum shell element. Three models with three different composite materials were assigned with their appropriate composite layups. The following materials were employed for the studies: (1) glass fiber-reinforced polymer such as S−Glass 913/Epoxy, (2) carbon fiber-reinforced polymer such as TC35/Epoxy and (3) M55/Epoxy.

The material properties given in Table 2 refers to previous experimental study conducted by Suwarta [11], where each material has a different ply thickness, resulting in different number of plies for each model. All plies were stacked in unidirectional from inner to outer part of the beam. Properties needed to simulate deflection are Elastic Young's Modulus (E), Poisson Ratio (ν) and Shear Modulus (G) as shown in Table 2. TC35/Epoxy and M55/Epoxy is chosen due to its longitudinal Young's modulus (E_{11}) and its thickness of around 0.03 mm which is consider as thin-ply. Thin-ply composites has the advantages of more degrees of freedom in fibre orientation leading to 'high definition' engineering and greater optimization [12]. Standard thickness S−Glass-913/Epoxy is chosen as there is a smaller number of plies used to produced the box spar as shown in Table 2 which could lead to much shorter production time and cheaper price.

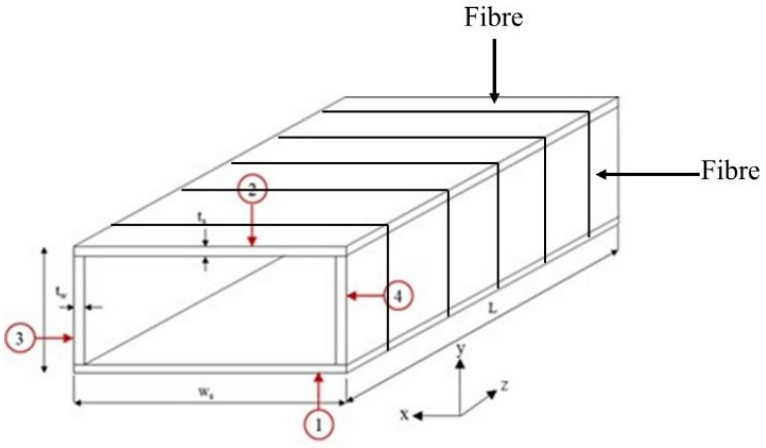

Figure 1. Partition in box spar structure: (1) Bottom spar cap, (2) Top spar cap, (3) Left shear web, (4) Right shear web.

2.2. Applied Boundary Conditions

In this section, the description of the boundary conditions will be given. The physical geometry was modeled in ABAQUS and boundary conditions were given to simulate the structural characteristics. The leftmost part of the beam representing the root part of the blade was given encastre boundary condition to simulate fixed support in a cantilever beam. In reality, this is partly correct because the blade has a zero-movement relative to the hub when it is deflected. However, more complex modeling strategy may include also the deflection of the tower and the entire

Table 1. Box spar dimension.

Component	Width (W) m	Thickness (ts,tw) m	Length (L) m
Spar Caps	0.800	0.060	102.880
Shear Web	0.576	0.040	102.880

Table 2. Material properties for S-Glass 913/Epoxy, TC35/Epoxy, M55/Epoxy.

Material	E_{11} (GPa)	E_{22} (GPa)	G_{12} (GPa)	ν_{12}	Ply Thickness (mm)	Number of Piles	
						Cap	Web
S-Glass 913/Epoxy	45.7	10.3	3.1	0.3	0.155	388	259
TC35/Epoxy	114.3	11	4.4	0.3	0.027	2223	1482
M55/Epoxy	280	6.3	3.1	0.31	0.030	2000	1334

turbine geometry, but this would be too expensive to be simulated.

As illustrated in Figure 2(a), fixed supports are shown with red markings around the root. The model was meshed as shown in Figure 2(b), where the distance between each node in the span length is about 1 m. Grid studies have been done to determine that this 1 m grid spacing is sufficient for computing the tip deflection of the blade as will be shown in Section 3.1.

Loads applied in the model were pressure derived from wind force simulated in AVATAR studies using CFD and BEM methods by Bangga [2]. In the present studies, the acting load is not directly simulated due to its non-linear characteristic and complex function, see Figure 3. Simplifications were made by applying trapezoidal rule to make approximation of the load into uniformly distributed load. The value of uniformly distributed load then derived into the value of aerodynamic pressure (in Pa) for each mesh point. The pressure point was applied at the top-most part of spar cap as illustrated in Figure 2(a) by red arrows pointing downwards, indicating the direction of the pressure applied to the spar.

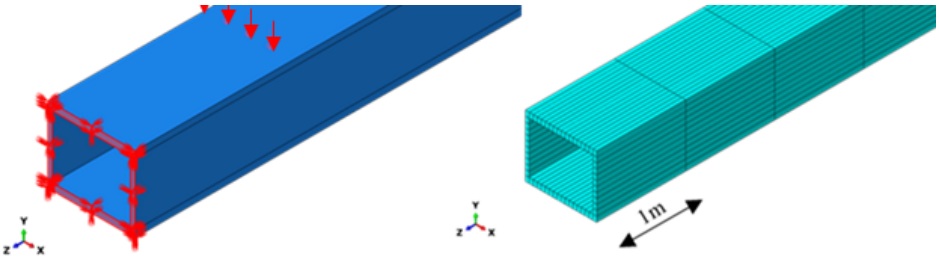

Figure 2. (a) Encastre boundary condition (b) Meshing in model.

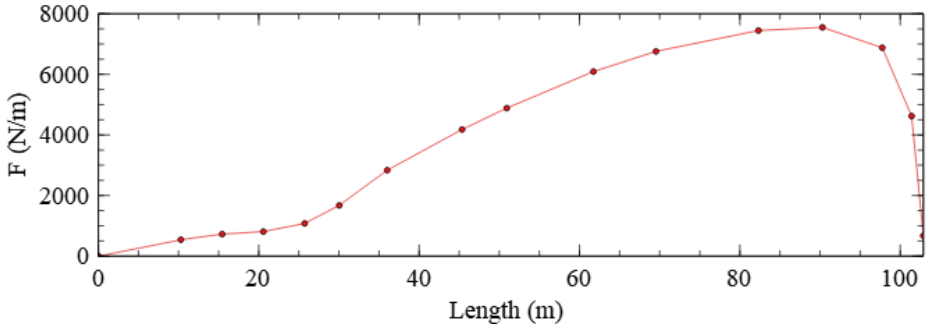

Figure 3. Wind force calculated by CFD (10.5 m/s) [2].

3. Results and Discussion

3.1. Grid Studies

Grid studies were done to determine appropriate number and size of elements to be meshed in all simulations. The results of studies are presented in Figure 4.

Initial study was done with total of 1456 elements (mesh size of 4 m) and this resulted in tip deflection of 2.54 m. Following grid studies were done by decreasing mesh size by 0.5 m at each study, hence increasing number of elements in the model. Figure 4 shows that two studies that have the smallest difference are grid studies with 5768 elements (mesh size of 1 m) and 11536 elements (mesh size of 0.5 m). While the number of elements is twice the size, the difference of tip deflection between the two studies are smaller compared to previous study in the 2000-4000 elements range, therefore it can be inferred that at the size of 0.5 – 1 m the mesh is already independent and will not have significant difference. In this study, the mesh size of 1 m was chosen due to shorter simulation time.

3.2. Deflection Characteristics

In this section, the characteristics of blade tip deflection will be discussed. The spar deflection is evaluated by its tip deflection (farthest point from the root and where it is not constrained) for each model. By comparing the result with existing tip deflection result from AVATAR studies, the results can be used to justify if materials used may be recommended for wind turbine blade.

The results from finite element analysis are presented in Table 3 and Figure 5. The deflection curve shown in Figure 5 shows that the deflection curve of the three composite materials having a similar non-linearity curve. It is shown that the nonlinearity increases from the root to the tip of the blade due to the absence of a fixed support especially at the tip of the blade. It can be seen that TC35/Epoxy has the smallest tip deflection out of three materials followed by S−Glass 913/Epoxy and the largest tip deflection is shown for M55/Epoxy. The M55/Epoxy composite material has the largest tip deflection among the others because the transverse Young's Modulus (E_{22}) of this material is 6.3 GPa which is small compared to E_{22} value of 10.3 GPa and 11 GPa for S−Glass/Epoxy and TC35/Epoxy respectively. The transverse Young's Modulus (E_{22}) plays an important role in determining the deflection performance because the fibre at the spar cap is arranged at 90° relative to the loading direction or to the x direction according to Figure 1. The load itself is acting on the spar cap at the y direction and when the spar is deflected, the deformation is mainly to the transverse direction or to the z direction according to Figure 1 which mean that the stiffness at the transverse direction plays an important role to resist the deformation. Although each model has the same boundary condition and geometry, but different results in deflection can be observed. Referring back to Table 2, it can be seen that S−Glass 913/epoxy and TC35/epoxy have relatively similar value of E_{22}, while the value of this property is much smaller for M55/Epoxy when compared to S−Glass 913/Epoxy and TC35/Epoxy. On the other hand, the value of E_{11} of each material varies, with S−Glass 913/Epoxy having the lowest value of 45.7 GPa and M55/Epoxy having the highest value of approximately six times higher. It can be inferred from this study that different material properties especially in the elastic modulus E_{11} and E_{22} could yield in different value of deflection. This claim will be analyzed further by comparing results from this study to the past study conducted by Croce et al. [13].

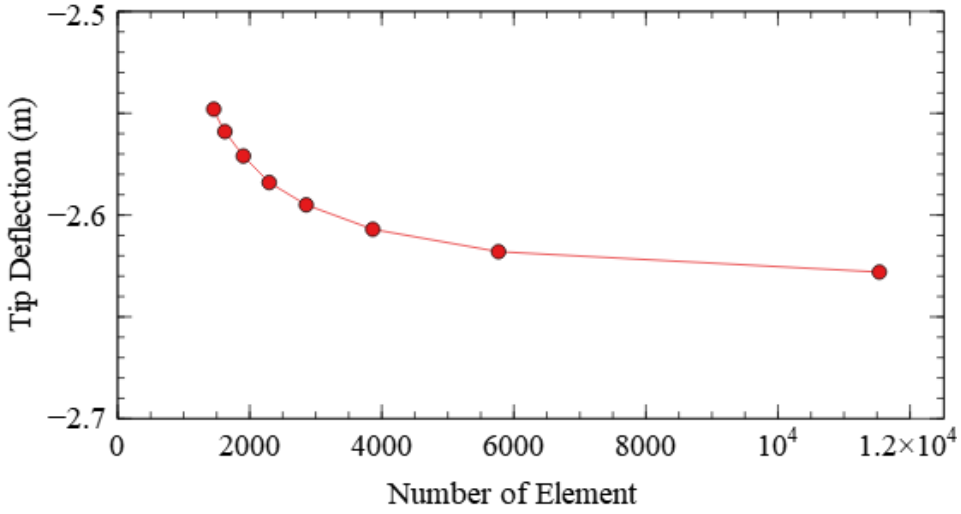

Figure 4. Grid studies results with S-Glass 913/Epoxy material.

Table 3. Maximum deflection on thickness S-Glass 913/Epoxy, TC35/Epoxy, M55/Epoxy and AVATAR wind turbine.

Material	Deflection (m)
S-Glass 913/Epoxy	2.618
TC35/Epoxy	2.429
M55/Epoxy	4.175
AVATAR	4.450

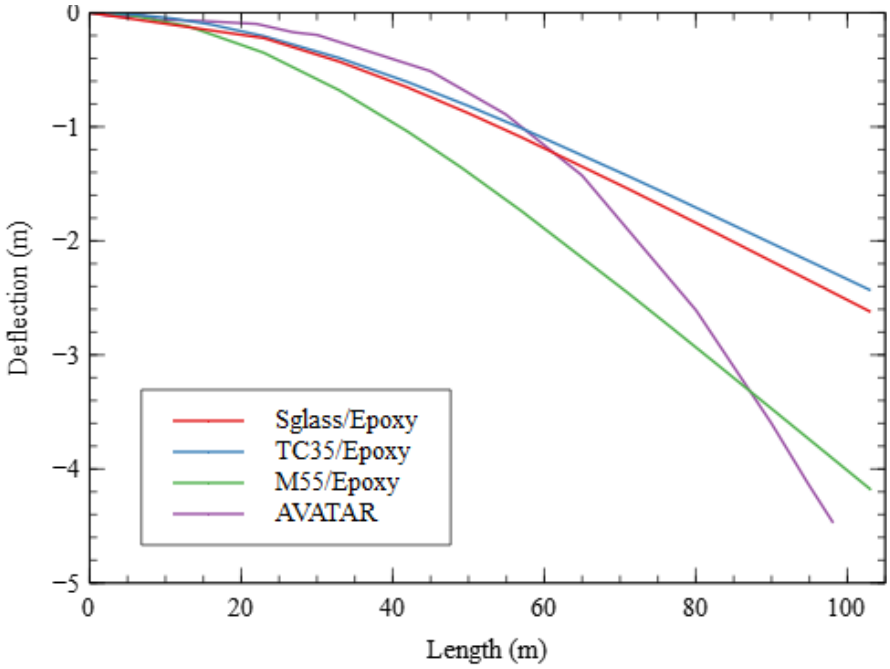

Figure 5. Deflection comparison.

While M55/Epoxy has the largest deflection out of three materials, it also has the smallest difference with AVATAR model with the difference of 0.275 m. It is important to note that the models used in this study and AVATAR study conducted by Croce et al. [13] are not the same, with few differences as shown in Table 4. Few things that contribute to the different value of deflection are; Croce et al. [13] simulated a higher wind speed of 11 m/s, and it is important to note that wind speed is proportional to deflection. Other than that, the materials used are totally different where Croce et al. [13] used unidirectional carbon fiber (uniaxial) combined with balsa for the spar caps, and biaxial material for the shear webs.

When compared to the elastic property of M55/Epoxy, it can be seen that uniaxial carbon fiber used in the AVATAR model from Croce et al. [13] has a similar value of elastic modulus E_{22}, while the E_{11} value of both materials is notably different (Table 5). The E_{11} value obtained from Croce et al. [13] is the closest to TC35/Epoxy with the difference of 0.7 GPa, but the value of deflection is almost twice as big. This proves that elastic modulus contributes a lot to the value of deflection, especially elastic property E_{22} in the transverse direction.

Table 4. AVATAR and box spar comparison.

Variable	Model	
	AVATAR	Box Spar
Wind Speed	11 m/s	10.5 m/s
Geometry	Airfoil with internal box structure(Polimi Redesign v.4)	Internal box structure INNWIND and Polimi Redesign v.r0 model
Material	UD Carbon fiber, Balsa, Triaxial	Unidirectional Ply S-Glass 913,TC35, M55

Table 5. Material properties of AVATAR Polimi Redesign v.4.

Property	Material		
	M55/Epoxy	Uniaxial (CF)	Biaxial
E_{11} (GPa)	280	115	13.92
E_{22} (GPa)	6.3	7.56	13.92
ν_{12}	0.31	0.3	0.533
G_{12} (GPa)	3.1	3.96	11.5

3.3. Stress Distribution Characteristics

It is important to note that the stress being analyzed is the maximum von-mises equivalent stress in the ply at the condition of maximum deflection, thus the location of maximum stress may vary within the thickness. Stresses in shear web and spar cap are analyzed at 11 different plies in each laminate, however only one part of each shear web and spar cap is analyzed as left-right shear web and top-bottom spar cap have similar values of stresses. Figure 6 and Figure 7 show the stress distribution along the thickness, where the plies are stacked from inner to outer part of the box spar. From the simulation results, the location with the highest stress concentration is located at the span within two meters from the root and the stress distributions are also analyzed.

It can be seen from Figure 6 and Figure 7 that there are several changes in the location of maximum stress (indicated by different nodes). The results show that M55/Epoxy has the highest stress both in shear webs and spar caps, while S−Glass 913/Epoxy has the smallest maximum stress. The trend in shear webs shown in Figure 7 indicates that maximum stress of shear webs rises from the inner to the outer part of shear web thickness.

The trends in spar cap (Figure 6) for each material are quite different, in M55/Epoxy it can be seen that there is no change in location of maximum stress within the ply (same node throughout the thickness). This is due to the high stiffness value of the material. On the other hand, S−Glass 913/Epoxy and TC35/Epoxy have similar trends. From inner to middle part, the maximum stress is declining and from the middle to outer part the maximum stress is rising. This phenomenon can be analyzed by looking at the location of the maximum stress in three plies (inner, middle, and outer) in the span within five meters from root for each material as shown in Figure 8.

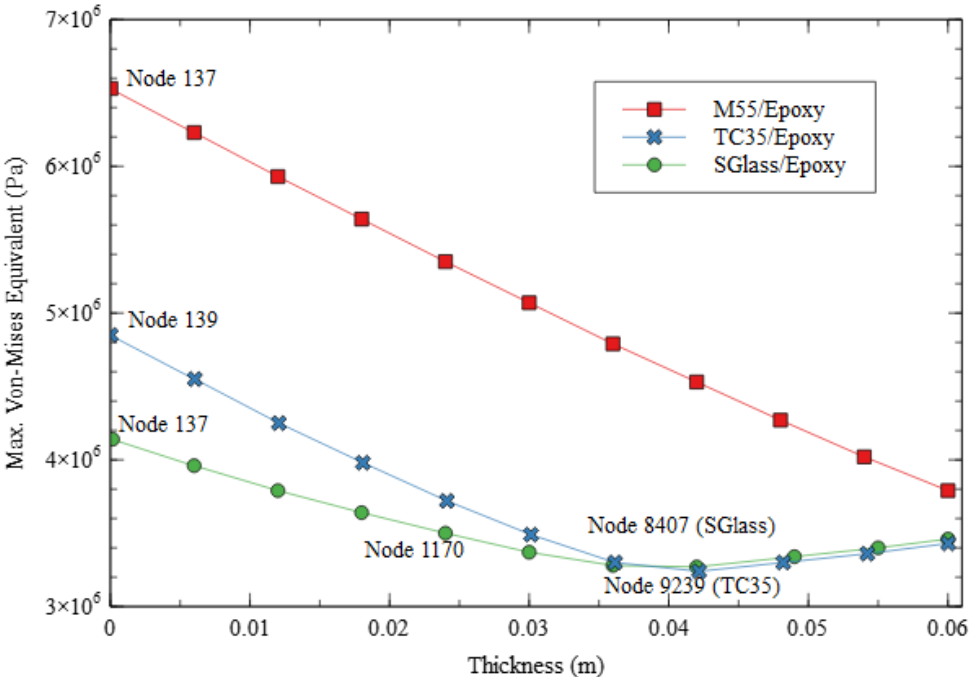

Figure 6. Stress distribution along the thickness in spar cap.

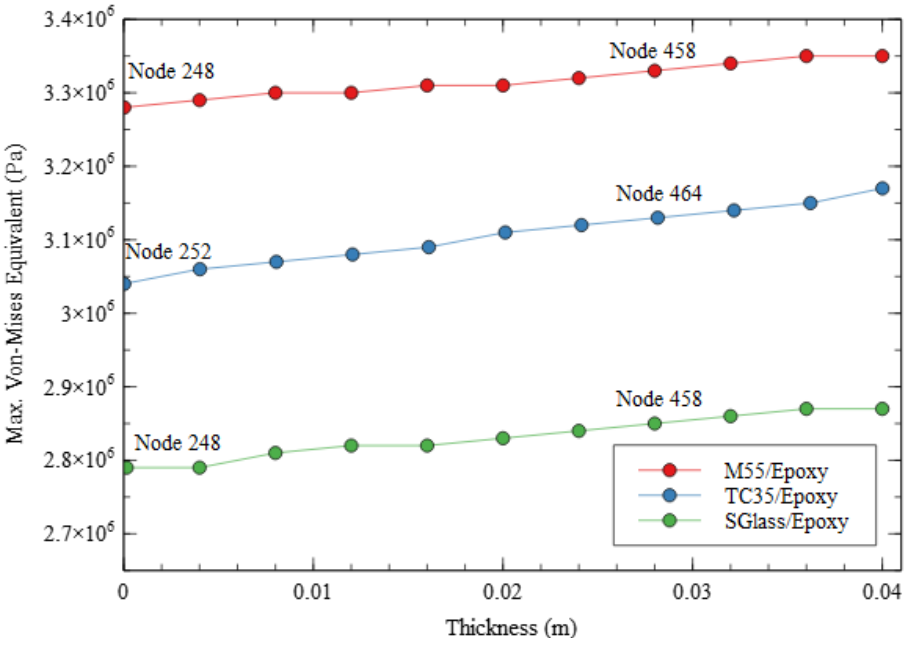

Figure 7. Stress distribution along the thickness in shear web.

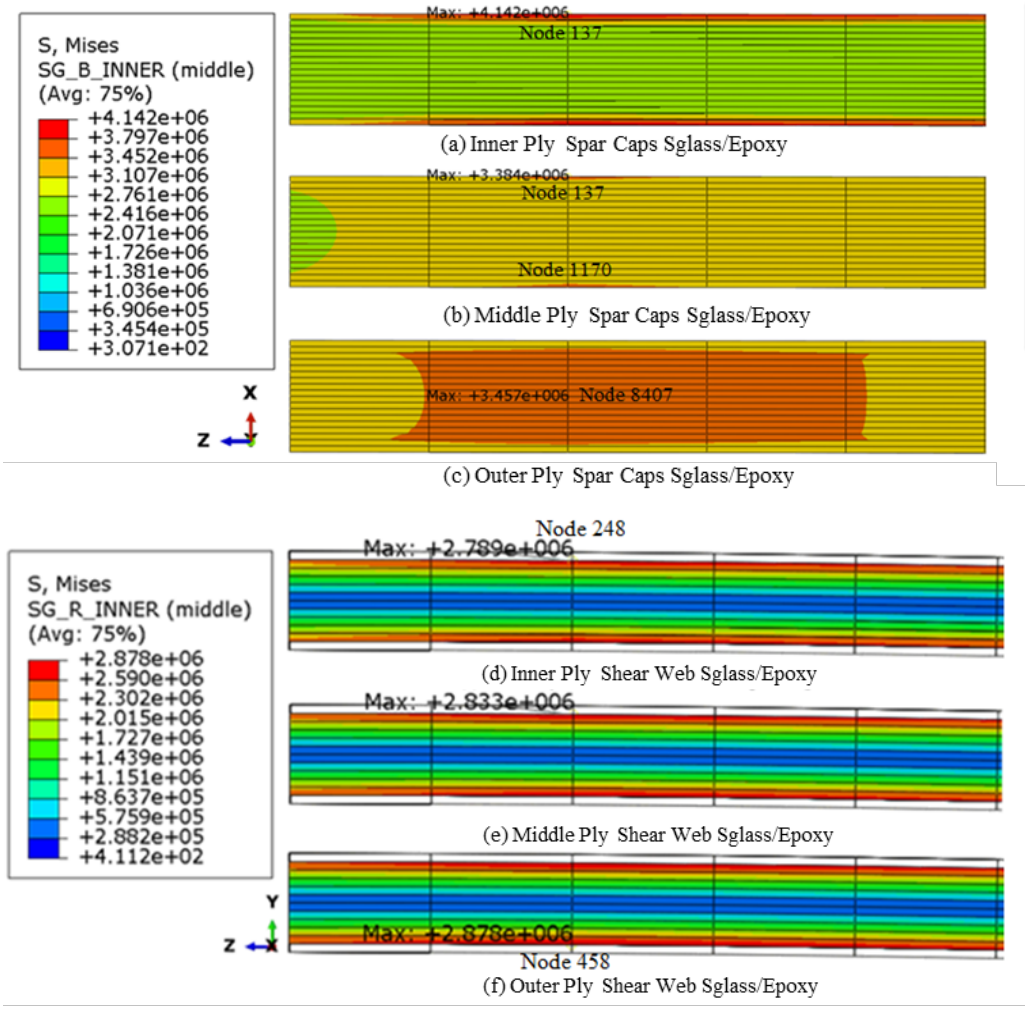

Figure 8. S-Glass material stress contours for shear web and spar cap.

From Figure 8(a)-(c), the stress contours in bottom spar cap for S−Glass 913/Epoxy material are shown from top (*y* direction). It can be seen that the maximum stress in inner ply (Figure 8(a)) is located at the area where spar cap supports the left part of the shear web (Node137), specifically in the area where stress transfer between shear web and spar cap occurs. Meanwhile, in the outer ply of S−Glass 913/Epoxy (Figure 8(c)) maximum stress is located at the surface free from supporting any left part of the shear web. It can also be seen that in node 137 (area that supports left part of the shear webs) the stress values are declining through the thickness as the contour turned from red (Figure 8(a)) to green (Figure 8(c)). The same trend also occurs for other materials, where the stress in the supporting area declines across the thickness, while the stresses in the non-supporting part are rising throughout the thickness. It can be seen from can be seen from Figure 8(d)-(f) that the right shear web is viewed from *x*-axis and has its maximum stresses located at the topmost and bottommost part where it is connected with the bottom and top spar caps.

The same thing can be seen for all three materials as shown in Figure 9(a)-(f) and Figure 10(a)-(f). Contrary to spar caps, the trend in shear web as shown in is that the maximum stresses at the interconnected part between the spar caps and shear webs increases from the inner part to the outer part.

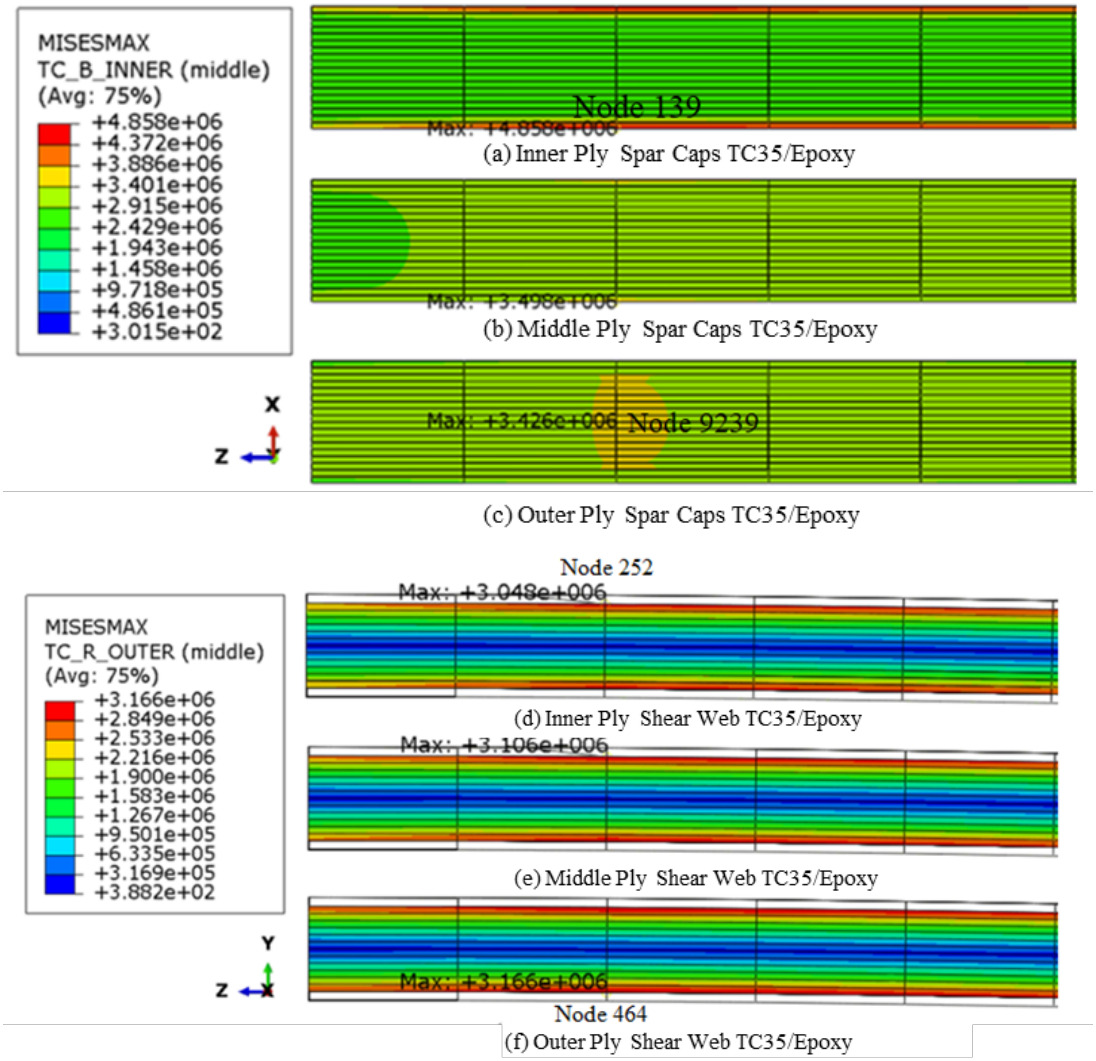

Figure 9. TC35/Epoxy material stress contours for shear web and spar cap.

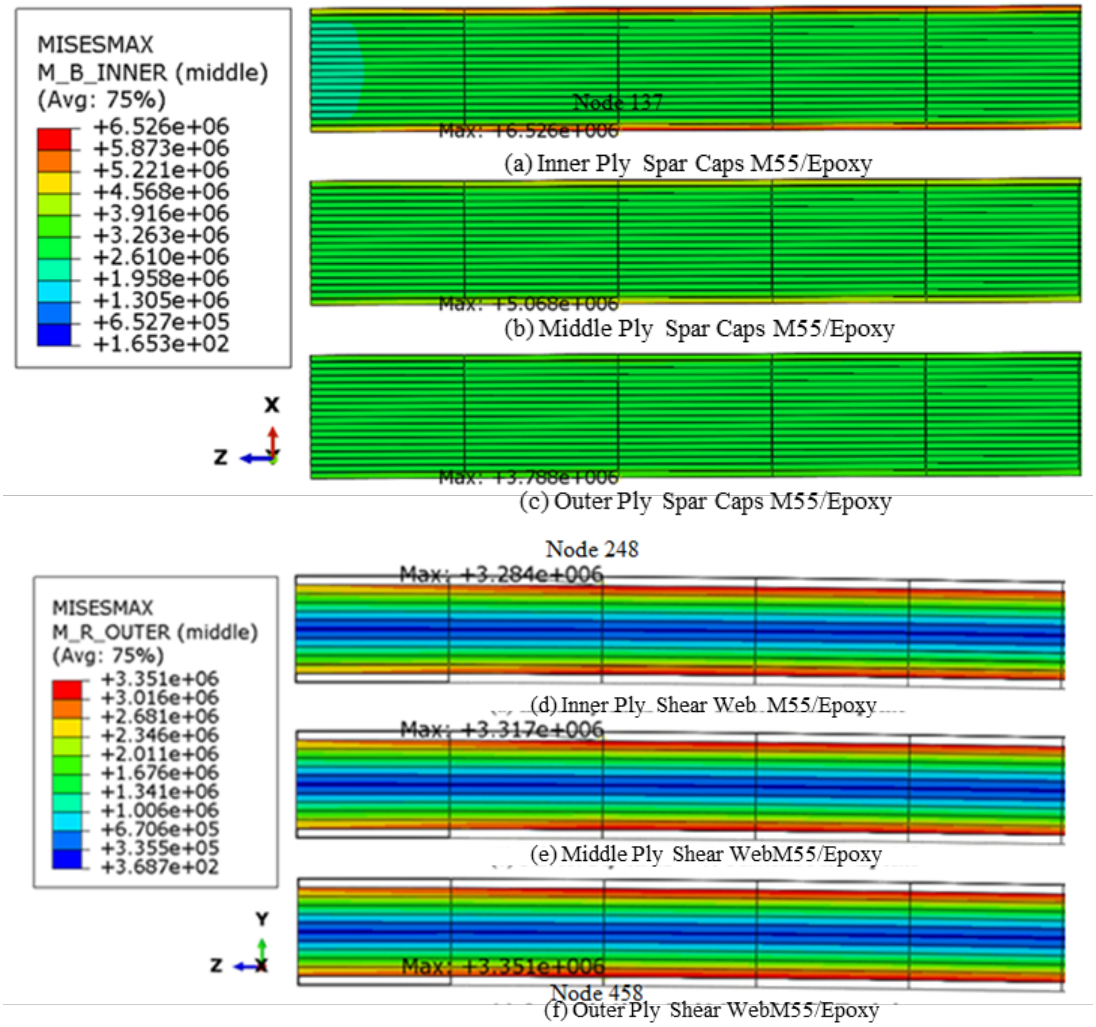

Figure 10. M55 material stress contours for shear web and spar cap.

Overall result shows that stresses in spar caps are higher than shear web, this is due to the difference in dimension, the number of plies, and spar location where spar caps received the load directly. Stresses in different materials also differ due to different value of elastic property, where in this case stiffness in longitudinal direction (E_{11}) plays an important role. A similar result was also found in the study by Nazha [14] where unidirectional carbon fiber resulted in higher stresses compared to glass fiber. However, with the results from the present study, it is not enough to determine whether current materials can be applied directly into wind turbine blade as the safety factors has yet to be determined. More experimental studies such as bending, tensile, and compression tests are needed to ensure these new composite materials could be useful for wind turbine blade design.

4. Conclusion

Numerical study to examine the deflection performance and stress distribution of wind turbine box spar has been performed. The effect of three different composite material's properties was examined. The deflection curve of the three composite materials showing nonlinear behaviour with a maximum deflection of 2.618 m, 2.429 m, 4.175 m at the blade tip for S−Glass 913/Epoxy, T35/Epoxy, M55/Epoxy respectively. The maximum deflection of those three composite materials is less compared to the maximum deflection of 4.450 m for the existing AVATAR beam showing the potential of the three composite materials.

The critical stresses are located at the top outer surface of the spar cap which received the load directly and at the intersection between the spar caps and shear webs where stress transfer occurs. The deflection performance for this study is dictated by the transverse Young's Modulus (E_{22}) of each material. The longitudinal Young's Modulus (E_{11}) plays an important role in determining the stress distributions. Materials with maximum equivalent von mises stress ranked from highest to lowest are: M55 Carbon/Epoxy, TC35 Carbon/Epoxy, and S−Glass 913/Epoxy.

References

[1] IEA, "World Energy Outlook 2019," 2019.

[2] G. Bangga, "Comparison of blade element method and CFD simulations of a 10 MW wind turbine," *Fluids*, vol. 3, no. 4, p. 73, 2018.

[3] G. Bangga, *Three-dimensional flow in the root region of wind turbine rotors*. kassel university press GmbH, July 2018.

[4] A. R. Ghasemi and M. Mohandes, "Composite blades of wind turbine: Design, stress analysis, aeroelasticity, and fatigue," *Wind turbines-design, control and applications*, vol. 4, no. 3, pp. 1–26, 2016.

[5] P. S. Veers, T. D. Ashwill, H. J. Sutherland, D. L. Laird, D. W. Lobitz, D. A. Griffin, J. F. Mandell, W. D. Musial, K. Jackson, M. Zuteck, *et al.*, "Trends in the design, manufacture and evaluation of wind turbine blades," *Wind Energy: An International Journal for Progress and Applications in Wind Power Conversion Technology*, vol. 6, no. 3, pp. 245–259, 2003.

[6] K. Cox and A. Echtermeyer, "Structural design and analysis of a 10 MW wind turbine blade," *Energy Procedia*, vol. 24, no. 1876, pp. 194–201, 2012.

[7] P. Prombut and C. Anakpotchanakul, "Deflection of composite cantilever beams with a constant i-cross section," in *IOP Conference Series: Materials Science and Engineering*, vol. 501, p. 012025, IOP Publishing, 2019.

[8] P. Chaviaropoulos, D. Lekou, D. Chortis, A. Irisarri, X. Munduate, K. Thomsen, H. Madsen, K. Yde, M. Reijerkerk, M. Stettner, *et al.*, "AVATAR Reference Blade Design," pp. 1–52, Nov. 2017.

[9] D. J. Peter Hjuler, Bacharoudis. K, Lekou. D.J., Makris. A., Dekker. J.P., Winkel. G.D., Croce. A., and Wang. D., "Deliverable 2.22 - new lightweight structural blade designs & blade designs with build-in structural couplings," pp. 1–21, Apr. 2014.

[10] P. Roth-Johnson, R. E. Wirz, and E. Lin, "Structural design of spars for 100-m biplane wind turbine blades," *Renewable Energy*, vol. 71, pp. 133–155, 2014.

[11] P. Suwarta, *Pseudo-ductility of unidirectional thin-ply hybrid composites*. PhD thesis, University of Bristol, 2020.

[12] J.C. Robin Amacher, W. Smith, C. Dransfeld, and J. Botsis, "Thin ply: from size-effect characterization to real life design," *Proceedings of the CAMX 2014 conference in Orlando, United States*, 2014.

[13] A.A. Croce, *et al.*, "Effect of blade flexibility and structural tailoring on loads," Nov. 2017.

[14] H. Nazha and Z. Aldeen, "A comparative study between Epoxy S-Glass UD and Epoxy Carbon UD for their use as manufacturing materials for wind turbine blades," pp. 33–41, June 2020.